Highly Sensitive and Selective Chip-Based Fluorescent Sensor for Mercuric Ion: Development and Comparison of Turn-On and Turn-Off Systems

ARTICLE *in* ANALYTICAL CHEMISTRY · SEPTEMBER 2012

Impact Factor: 5.64 · DOI: 10.1021/ac301954j · Source: PubMed

8 AUTHORS, INCLUDING:

Meiying Liu
Chinese Academy of Sciences
20 PUBLICATIONS **550** CITATIONS
SEE PROFILE

Xinhui Lou
Capital Normal University
35 PUBLICATIONS **1,126** CITATIONS
SEE PROFILE

Zhao Jianlong
Chinese Academy of Sciences
120 PUBLICATIONS **1,207** CITATIONS
SEE PROFILE

analytical chemistry

Article

pubs.acs.org/ac

Highly Sensitive and Selective Chip-Based Fluorescent Sensor for Mercuric Ion: Development and Comparison of Turn-On and Turn-Off Systems

Juan Du,[†,∥,⊥] Meiying Liu,[†,∥,⊥] Xinhui Lou,*[,‡,⊥] Tao Zhao,[‡] Zheng Wang,[§] Ying Xue,[§] Jianlong Zhao,[†] and Yuanshen Xu[†]

[†]State Key Laboratory of Transducer Technology, Shanghai Institute of Microsystem and Information Technology, Chinese Academy of Science, Changning Road 865, Shanghai, China 200050

[‡]Department of Chemistry, Capital Normal University, Xisanhuan North Road 105, Beijing, China 100048

[§]Beijing Municipal Center for Disease Prevention and Control, HePingLi Middle Street 16, Beijing, China 100013

[∥]Graduate School of the Chinese Academy of Sciences, Beijing, China 100049

Supporting Information

ABSTRACT: Miniaturization is currently an important trend in environmental and food monitoring because it holds great promise for on-site monitoring and detection. We report here two ready-to-use chip-based fluorescent sensors, compatible with microarray technology for reagentless, one-step, fast, highly sensitive and selective detection of the mercuric ion (Hg^{2+}) in the turn-on and turn-off operation modes. Both operation modes are based on the highly selective T−Hg^{2+}−T coordination between two neighboring polythymine (T) strands at a high probe density and its induced displacement of the complementary polyadenine strand labeled with either fluorophore or quencher, which enables the turn-off and turn-on detection of Hg^{2+}, respectively. The turn-off sensor is slightly more sensitive than the turn-on sensor, and their detection limits are 3.6 and 8.6 nM, respectively, which are both lower than the U.S. Environmental Protection Agency limit of [Hg^{2+}] for drinkable water (10 nM, 2 ppb). Compared to the turn-off sensor with the dynamic Hg^{2+} detection range from 3.6 nM to 10 μM (R^2 = 0.99), the turn-on sensor has a broader dynamic Hg^{2+} detection range, from 8.6 nM to 100 μM (R^2 = 0.996). Both sensors exhibited superior selectivity over other reported sensors using thymine-rich probes for Hg^{2+} detection over other common metal ions. In addition, the practical application of the chip-based sensors was demonstrated by detecting spiked Hg^{2+} in drinking water and fresh milk. The sensor has great potential for on-site practical applications due to its operational convenience, simplicity, speed, and portability.

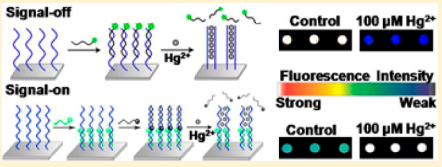

Mercury is a bioaccumulative and highly toxic heavy metal that causes serious human health problems even at low concentrations.[1,2] The solvated divalent mercuric ion (Hg^{2+}) is one of the most common and stable forms of mercury pollution due to its high water solubility. Because of continuing concern over mercury contamination in the environment and food, obtaining new mercury detection methods that are cost-effective, rapid, facile, sensitive, selective, and applicable to on-site detection is an important goal. Traditional analytical techniques for Hg^{2+} quantification, such as atomic absorption/emission spectroscopy, selective cold vapor atomic fluorescence spectrometry, and inductively coupled plasma mass spectrometry (ICP-MS), are very sensitive and selective but require expensive and sophisticated instrumentation which limits their application in on-site Hg^{2+} monitoring.[3] Intended for on-site detection, many molecular probe-based sensors using organic chromophores,[4] small fluorescent organic molecules,[5] conjugated polymers,[6] proteins,[7] oligonucleotides,[8−10] DNAzymes,[11] and antibodies[12] have been developed for fluorescent,[8,9,11,13−20] colorimetric,[21−27] and electrochemical[28−31] detection of Hg^{2+} in aqueous solution. On-site applications require methods with good sensitivity, good selectivity, reliability, and, especially, simple operation. Most sensors reported so far, however, are not suitable for on-site applications due to various reasons such as poor aqueous solubility, bad stability, low sensitivity, cross-sensitivity toward other metal ions, and the requirement of multistep operations. Thus, the development of highly sensitive, selective, and ready-to-use methods for aqueous Hg^{2+} remains a challenge.[5]

Miniaturized technologies, especially microchips, have been widely applied for gene[32] and protein[33] analyses mainly due to their high-throughput, easy operation, and good reliability. Miniaturization is currently an important trend in environmental and food monitoring because it holds great promise for on-site monitoring and detection. The chip-based sensors are technically compatible with miniaturization technologies. Several chip-based methods using polymer matrices,[34,35] oligopeptide-modified silicon nanowires,[36] DNAzyme,[37−39] proteins,[40−42] and oligonucleotides[43] have been

Received: July 12, 2012
Accepted: August 27, 2012
Published: September 7, 2012

   dx.doi.org/10.1021/ac301954j | *Anal. Chem.* 2012, 84, 8060−8066

reported for metal ion analyses. However, very few chip-based sensors for Hg^{2+} detection have been developed so far. Use of a plate-based colorimetric sensor has achieved submicromolar sensitivity for Hg^{2+} detection using a mesoporous nanocrystalline TiO_2 film sensitized with a ruthenium dye.[44] However, the U.S. Environmental Protection Agency (EPA) limit of acceptable Hg^{2+} concentration in drinkable water is 10 nM (2 ppb). The sensor provides the convenience of the colorimetric assay but is not sensitive enough for practical applications. Mirkin et al.[43] developed a chip-based scanometric assay for the detection of Hg^{2+} based on the sharp melting properties of DNA–AuNPs and the selective T–Hg^{2+}–T coordination chemistry, resulting in the stabilization of the duplex.[8,45,46] The sensor has multiple strengths over other chip-based sensors, including good stability,[47] simple sensor preparation, easy chemical engineering and modification, high selectivity, and high sensitivity (10 nM, or 2 ppb). This sensor system, however, displayed drawbacks in terms of actual applicability, such as the requirement of an electronic heating element for careful monitoring of the thermal denaturation temperature and silver enhancement for signal amplification during the detection process.

In this work, we designed a chip-based fluorescent sensor for detection of Hg^{2+} in aqueous solutions that utilized the selective T–Hg^{2+}–T coordination between two neighboring polythymine strands and its induced displacement of the fluorophore- or quencher-labeled polyadenine strand in the turn-off and turn-on platform, respectively. Both the turn-off and the turn-on sensors have sensitivities below the EPA limit of acceptable Hg^{2+} concentration in drinking water. Both sensors exhibit superior selectivity over other reported sensors using thymine-rich probes for Hg^{2+} detection over other metal ions. Importantly, the ready-to-use sensor not only has the inherent advantages of oligonucleotide-based sensors like the scanometric sensors described above but also has the great practical applicability due to its reagentless and one-step simple operation. The sensor was also tested to detect Hg^{2+} spiked in drinking water and fresh milk to demonstrate its potential for practical applications.

EXPERIMENTAL SECTION

Materials. Silyated slides (aldehyde) were purchased from CEL Associates, Inc. (Pearland, TX). The 2× spotting solution was purchased from TeleChem International Inc. Oligonucleotides were synthesized and purified by Takara Biotechnology Co. (Dalian, China). The oligonucleotide sample names and sequences are given in Figures 1 and 2. 3-(*N*-Morpholino)-propanesulfonic acid (MOPS) was purchased from Sigma. Standard mercury in 2–5% nitric acid was purchased from AccuStandard. The Hg^{2+} stock solution was diluted to the desired concentration with the MOPS buffer (100 mM $NaNO_3$, 10 mM MOPS, pH 7.2). All other reagents were of analytical grade. All solutions were prepared with Milli-Q water (18.2 MΩ cm^{-1}) from a Millipore system.

Preparation of the Oligonucleotide Chip Array. Both the turn-off and turn-on chip arrays were prepared as follows: 5′-amine-modified single-strand oligonucleotide, probe A (Figure 1) or probe A′ (Figure 5), was dissolved with Milli-Q water and mixed with the same volume of the 2× spotting solution. The mixture was spotted onto the aldehyde-coated glass slides with a commercial arrayer (Cartesian, Pixsys 7500). After the spotting process, the oligonucleotide array was fixed at 25 °C for 48–72 h. Then, the oligonucleotide-arrayed slides were immersed in a 0.2% SDS solution for 2 min and rinsed with Milli-Q water for 2 min. Subsequently, the slides were treated with an aldehyde blocking solution (1 g of $NaBH_4$, 300 mL of phosphate buffer saline (pH 7.4), 100 mL of 99% ethanol) for 15 min and rinsed sequentially with a 0.2% SDS solution and Milli-Q water for 2 min each, followed by air drying for 30 s.

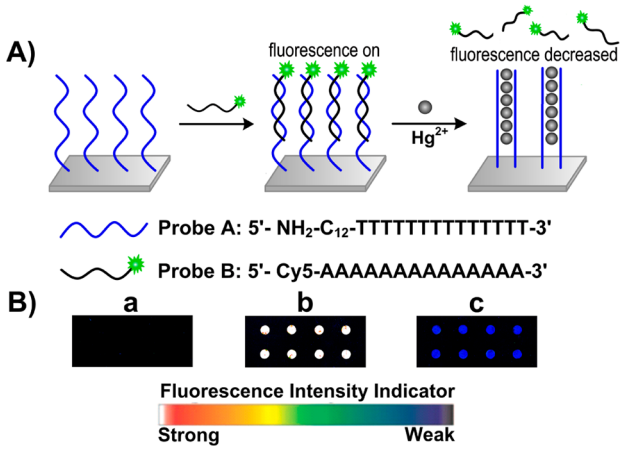

Figure 1. (A) Schematic of the turn-off chip-based fluorescent mercury sensor design. (B) The typical scanometric images of the slide after (a) immobilization of probe A (5 μM), (b) hybridization with probe B (2 μM), and (c) subsequent exposure to 100 μM Hg^{2+} for 1 h.

Preparation of the Turn-Off Fluorescent Sensor. The fluorophore-labeled oligonucleotide, probe B (Figure 1), was immobilized onto the chip via hybridization between probe B and probe A that was functionalized on the chip in the previous step. In brief, probe B was dissolved in the MOPS buffer to make a 2 μM solution. Hybridization on oligonucleotide-arrayed slide was carried out by placing the probe B solution onto the probe A spots, followed by covering a coverslip and leaving it overnight in a humid chamber at room temperature. The chip was then rinsed and soaked in the MOPS buffer for 5 min to remove nonspecifically adsorbed probe B. Finally, the chip was dried and stored in the dark in a humid chamber at 4 °C.

Preparation of the Turn-On Fluorescent Sensor. First, the fluorophore-labeled oligonucleotide, probe B′ (Figure 5), was immobilized onto the chip in the same way as probe B. The chip was then rinsed and soaked in the MOPS buffer for 5 min to remove nonspecifically adsorbed probe B′. After that, the quencher-labeled oligonucleotide, probe C′ (Figure 5), was immobilized onto the chip via hybridization in the same way. The chip was rinsed and stored in the dark, in the same way as described above for the turn-off sensor.

Scanometric Detection of Mercury(II) in the Buffer. Aliquots of various concentrations of Hg^{2+} were prepared from one concentrated Hg^{2+} stock solution (5 mM, determined by atomic absorption spectroscopy) by serial dilution in the MOPS buffer. The Hg^{2+} solutions were added to the six-well hybridization chambers assembled with the turn-off and turn-on chips separately and reacted at room temperature for various amounts of time. The chamber was then disassembled, and the slides were rinsed with the MOPS buffer for 5 min. Finally, the slides were imaged using a fluorescence scanner (General Scanning, Scanarray 3000) at 635 nm, and fluorescence intensity was calculated from the image using software written in-house. To investigate the selectivity of the assay, other metal

dx.doi.org/10.1021/ac301954j | Anal. Chem. 2012, 84, 8060–8066

ions (Ni^{2+}, Cu^{2+}, Zn^{2+}, Ca^{2+}, Mg^{2+}, and Pb^{2+}) at 10 μM were tested in the same way.

Scanometric Detection of Spiked-In Mercury(II) in Drinking Water. Aliquots of the drinking water were spiked with a concentrated stock solution of Hg^{2+}. Next, the concentrated MOPS and $NaNO_3$ solutions were added to the mixtures. The final concentrations of Hg^{2+}, MOPS, and $NaNO_3$ were 0.5 or 5 μM, 10 mM, and 100 mM, respectively. The scanometric detection of Hg^{2+} was then performed in a manner identical to that used for the buffer samples (vide supra).

Scanometric Detection of Mercury(II) in Fresh Milk. Two milliliters of fresh whole milk (bought from the grocery store) was mixed with 2 mL of concentrated Hg^{2+} solution (5 mM), followed by the addition of 4 mL of 65% HNO_3. The mixture was incubated at 95 °C for 2 h and then cooled to room temperature. Solid NaOH was subsequently added to the solution to adjust the pH to a range of 7−8. After centrifugation, the clear supernatant was collected and the concentrations of Na^+ and MOPS were adjusted to 100 and 10 mM, respectively, by dilution and the addition of a concentrated MOPS solution. The calculated final concentration of Hg^{2+} was 20 μM, assuming the spiked Hg^{2+} was 100% extracted by acid digestion. The scanometric detection of Hg^{2+} was then performed in a manner identical to that used for the buffer samples (vide supra). The milk without spiked Hg^{2+}, treated in the same manner, was used as a negative control.

Measurement of [Hg^{2+}] in Fresh Milk Using ICP-MS. ICP-MS measurements were performed by an Agilent 7500ce ICP-MS instrument (Agilent Technologies Inc., Santa Clara, CA) equipped with a Babington high-salt nebulizer. The calibration curve was obtained where the Hg^{2+} ion concentration ranged from 0 to 50 ppb in a matrix of a 5% HNO_3 solution, 1 ppb indium (internal standard), and nanopure water. The acid-digested sample prepared as described above was diluted 120-fold in the same matrix for ICP-MS measurements. Measured values were quantified by comparison to a standard curve that was generated from known concentrations of the Hg^{2+} ion in the same matrix.

RESULTS AND DISCUSSION

As shown in Figure 1A, the turn-off sensor system is comprised of two oligonucleotide strands; one is a 14-mer polythymine oligonucleotide (referred to as probe A) with an amine moiety at the 5′-end for surface attachment, and the other is a 14-mer polyadenine, probe B, with a fluorescent dye tag at the 5′-terminus. The design of the probes was based on the following considerations: First, the polythymine probe could provide better selectivity for Hg^{2+} detection than the thymine-rich probes since only T−Hg^{2+}−T coordination was specific to Hg^{2+}, and the presence of other complementary bases would decrease the selectivity.[22] Second, the shorter probes are preferable to the longer probes (such as structure-switching probes[13,31]) for more efficient surface immobilization, surface hybridization, and strand displacement due to the significantly decreased steric hindrance, probably resulting in more sensitive detection of Hg^{2+}. Finally, the length of the probes was selected as 14-mer to ensure effective surface hybridization for sensor preparation (the calculated melting temperature was 35.5 °C in the presence of 100 mM Na^+) and to minimize the chance of intramolecular T−Hg^{2+}−T coordination, which usually requires longer probes for conformational changes.[13,31] Upon the basis of this design, we assumed that the dominant mercury ion recognition mechanism at high probe density would be the T−Hg^{2+}−T coordination between two neighboring polythymine strands and its induced displacement of the fluorophore-labeled polyadenine strand. Upon addition of the Hg^{2+} solution, Hg^{2+} coordinates directly with the N3 of thymine and bridges two thymine residues in the two neighboring probe A strands to form the T−Hg^{2+}−T pair through covalent N−Hg^{2+} bonds.[46] Hg^{2+} binding to the DNA strand is a synergistic process, and the binding of one Hg^{2+} facilitates the binding of another Hg^{2+} to the same strand.[48] Also, the stability of this T−Hg^{2+}−T pair is higher than that of a T−A Watson−Crick pair.[45] Therefore, the formation of intermolecular T−Hg^{2+}−T base pairs between two probe A strands disrupts the double helix structure between probe A and probe B. As a result, the Cy5-tagged probe B is released from the chip surface with the fluorescence intensity substantially decreased.

First, we tested the feasibility of the proposed design. To construct the turn-off sensor, probe A was first covalently immobilized on the aldehyde-activated glass slide. Probe B labeled with the Cy5 tag was then hybridized with the immobilized probe A to prepare the sensor with a strong fluorescence. Note, Cy5 was selected as the dye in this study due to its superior brightness, good photostability, and relative water solubility.[49] The ready-to-use sensor was then tested in a 100 μM Hg^{2+} solution. The typical scanometric images of the slide after immobilization of probe A, hybridization with probe B, and subsequent exposure to a Hg^{2+} solution are shown in Figure 1B. The slide immobilized only with probe A showed no fluorescence. After hybridization, strong fluorescent spots were observed, implying that a 12 methlyene spacer of probe A was sufficient to facilitate the hybridization on an array, and Cy5-tagged probe B had successfully hybridized with probe A. Upon addition of the Hg^{2+} solution, a more than 93% decrease in the fluorescence of the spots was achieved, indicating that the sensor was responsive to Hg^{2+} as expected.

In order to further clarify whether or not the dominant mechanism of mercury ion detection of our sensor is the intermolecular T−Hg^{2+}−T coordination between two neighboring polythymine strands and its induced displacement of the fluorophore-labeled polyadenine strand (Figure 1A), several control experiments were conducted. First, the fluorescence intensities of probe B in the buffer solution were measured before and after adding 100 μM Hg^{2+} (final concentration). Only a less than 2.5% decrease of the fluorescence intensity was observed (Figure S-1 of the Supporting Information), which implied that the fluorescence decrease was not due to the direct quenching of the fluorescence of Cy5 by Hg^{2+}. Second, we explored the effect of the probe-to-probe spacing of probe A on the glass side surface on the relative fluorescence intensity decrease. If the intermolecular T−Hg^{2+}−T coordination was dominant, the sensor would show a decreased response at lower probe densities that would reduce the possibility of neighboring interactions. In contrast, if the intramolecular T−Hg^{2+}−T coordination allowing for ssDNA poly-T to fold onto itself was to still occur, it should be more efficient at lower probe densities due to the weakened steric interactions.[13,31] A series of sensors with gradually decreased probe density (or increased probe-to-probe spacing) was prepared by spotting probe A at various concentrations from 0.5 to 5 μM on the chip surface. When these sensors were challenged with the same concentration of Hg^{2+} (10 μM), percentage drops of the fluorescence intensity (the individual control signal as 100%) ranging from 88% to 36% were observed as the probe densities were decreased (Figure 2). This observation clearly indicated

dx.doi.org/10.1021/ac301954j | Anal. Chem. 2012, 84, 8060−8066

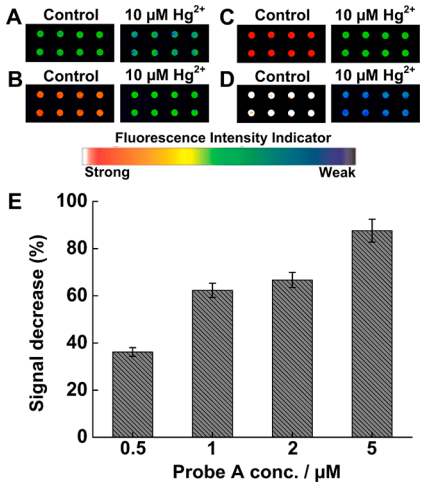

Figure 2. Scanometric images of the turn-off chip prepared by spotting probe A at (A) 0.5 μM, (B) 1 μM, (C) 2 μM, and (D) 5 μM before and after incubation with 10 μM Hg^{2+} for 1 h. (E) The percentage of fluorescence intensity decreases as a function of the probe A concentration. The illustrated error bars represent the standard deviation obtained from 8 data points.

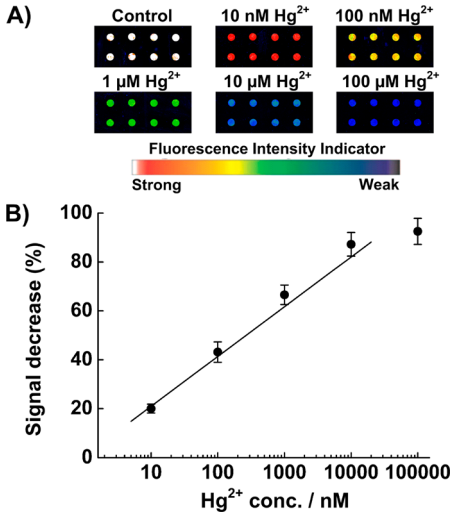

Figure 3. (A) Scanometric images of the turn-off chip in the presence of various concentrations of Hg^{2+} in the buffer. (B) The percentage of fluorescence intensities decreases as a function of the Hg^{2+} concentration in the buffer. The illustrated error bars represent the standard deviation obtained from 8 data points.

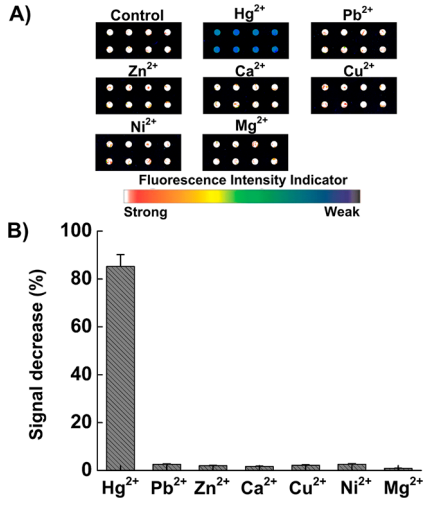

Figure 4. (A) Scanometric images of the turn-off chip in the presence of various metal ions at a concentration of 10 μM. (B) The percentage of fluorescence intensities decreases as a function of various metal ions.

that the intermolecular T−Hg^{2+}−T interaction was the dominant mechanism of the sensor at the high probe density that we used for our sensor in this work (5 μM probe A). It can be expected that the intramolecular T−Hg^{2+}−T interaction should be dominant at a low probe density. However, the absolute fluorescence is too weak for practical applications. Besides, the limited length of probe A (14-mer) could also prohibit the formation of an intramolecular hairpin structure. Finally, we designed structure switching probes D (5′-NH_2-C_{12}-GTTTGTTTGTTGGCCCCCTTCTTTCTTATCATCA-3′) and E (5′-Cy5-TGA TGA TAA GAA-3′), that is complementary to the 3′-end of probe D, to replace probes A and B, respectively. Under the same conditions, only a 35% fluorescence intensity decrease was observed after incubation for 1 h with 100 μM Hg^{2+}, and no signal decrease was observed when the sensor was challenged with Hg^{2+} with a concentration of less than 10 μM. The significantly higher detection limit might be caused by the steric hindrance problem on the surface. This observation further confirmed that our sensor did indeed function mainly via intermolecular T−Hg^{2+}−T interaction.

The response of the sensor to Hg^{2+} was prompt. The fluorescence intensity decreased by 45% and 63% only after incubation for 2 min with 10 and 100 μM Hg^{2+}, respectively. Around 95% response of the sensor to Hg^{2+} was achieved within 20 min (Figure S-2 of the Supporting Information). Our chip-based fluorescent Hg^{2+} sensor was very sensitive. A linear correlation existed between the signal decrease and the concentration of Hg^{2+} over the range of 0.01−10 μM (R^2 = 0.98) (Figure 3). The calculated detection limit (3 times the standard deviation of the blank) was 3.6 nM. The detection limit is lower than the EPA-permitted toxicity level of Hg^{2+} in drinking water (10 nM, or 2 ppb). The selectivity of the sensor was then determined by testing a spectrum of metal ions, including Ni^{2+}, Cu^{2+}, Zn^{2+}, Ca^{2+}, Mg^{2+}, and Pb^{2+}, respectively, all at a concentration of 10 μM (Figure 4). In contrast to a significant fluorescence decrease (85.2 ± 4.9%) as observed for Hg^{2+}, very little change (<2.6%) of the fluorescence intensity was observed upon exposure to other metal ions. The sensor showed superior selectivity over other sensors using thymine-rich probes.[13,22,29,31] In comparison, an optical Hg^{2+} sensor[22] recently reported by Willner's group, under the same metal ion concentrations (10 μM), showed a more than 40% signal change from Pb^{2+}, and 2,6-pyridinedicarboxylic acid was added to decrease the interference down to 10%. Other metal ions, including Ni^{2+}, Ca^{2+}, and Mg^{2+}, also caused around 10% strong interference. An electrochemical[31] sensor based on a structure-switching probe possessed improved selectivity for Ca^{2+} and Mg^{2+}; however, still a more than 10% signal change from Pb^{2+} and Cu^{2+} and a more than 5% negative singal change from Ni^{2+} were observed.

We reasoned that the significantly improved selectivity was due to two factors. First, the probe A used in our sensor is composed of thymine bases only, which are highly specific to Hg^{2+} by forming the T−Hg^{2+}−T base pair. An improved selectivity over most metal ions was reported recently by utilizing a polythymine probe for electrochemical Hg^{2+} detection.[29] However, their sensor suffered from very strong

dx.doi.org/10.1021/ac301954j | Anal. Chem. 2012, 84, 8060−8066

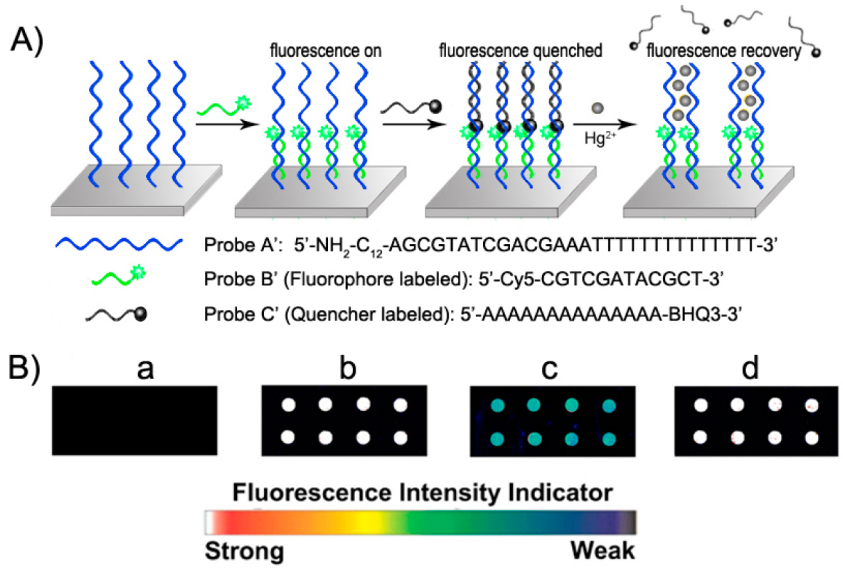

Figure 5. (A) Schematic of the turn-on chip-based fluorescent mercury sensor design. (B) The typical scanometric images of the slide after (a) immobilization of probe A′ (5 μM), (b) hybridization with probe B′ (2 μM), (c) hybridization with probe C′ (2 μM), and (d) subsequent exposure to 100 μM Hg^{2+} for 1 h.

interference from Cu^{2+} (around 100%). The authors reasoned that the exceptional interference from Cu^{2+} might be attributed to the formation of a complex between Cu^{2+} and T with a concomitant compact conformation for the poly-T probes. The interference was then eliminated by adding 20 mM adenine to the sample, which could coordinate with Cu^{2+} but not with Hg^{2+}. Second, the extra energy required for the subsequent strand displacement also contributed to the improved selectivity. The improved selectivity has been demonstrated by the sensors based on structure-switching probes.[13,31] In addition, in our sensor, probe B is composed of adenine bases, which could coordinate with Cu^{2+} after strand displacement to minimize the interference from Cu^{2+}. The excellent selectivity signified the potential of the sensor for Hg^{2+} detection in real samples.

To evaluate the practical applicability of the chip-based sensor, we used the sensor to detect Hg^{2+} spiked in drinking water. The exact same fluorescence intensity changes were observed for the samples containing Hg^{2+} at 0.5 μM (or 5 μM) in the buffer and the drinking water spiked with equivalent amounts of Hg^{2+}. The scanometric images and quantitative fluorescence changes can be found in Figure S-3A,B of the Supporting Information. We further explored the ability of the sensor to detect Hg^{2+} in food samples using fresh whole milk (China Mengniu Dairy Company Limited, China) bought from the grocery store. To the best of our knowledge, so far no sensor is able to directly detect mercury(II) in complex food samples due to the fact that Hg^{2+} forms stable chelated structures with the thiol and other functional groups of proteins in food. Therefore, time-consuming or complicated sample preparation procedures, such as microwave-assisted acid digestion, have to be used before mercury detection.[50] Our data confirmed that spiked-in Hg^{2+} in fresh milk without any pretreatment was not able to be detected by our sensor as shown in Figure S-3C of the Supporting Information. To broaden the potential applications of the sensors, the development of simple and fast sample pretreatment technologies is quite challenging and in urgent need. For this purpose, in this work we adopted very simple sample pretreatment steps to test the potential of our sensor for on-site applications. There was no detectable Hg^{2+} in the original milk by ICP-MS. $Hg(NO_3)_2$ was added to a 2 mL aliquot of milk followed by the addition of concentrated HNO_3. The mixture was then treated by simple incubation and centrifugation as described in the Experimental Section. After the treatment, the theoretical concentration of Hg^{2+} was 20 μM, assuming the extraction efficiency was 100%. The sample was then detected by our sensor, and a 72% fluorescence intensity decrease (Figure S-3C of the Supporting Information) was observed, which corresponds to 3.2 μM Hg^{2+} from the calibration curve in Figure 3B. As expected, this value was smaller than the theoretical value due to the lower Hg^{2+} extraction efficiency of the simplified sample treatment methods. To confirm the reliability of this value, the same sample was detected by ICP-MS and the measured value was 2.8 μM, which was compatible with the value obtained by our sensor, demonstrating the potential application of our sensor for on-site detection of Hg^{2+} in food samples. The slightly lower value obtained by ICP-MS could be due to the inefficient formation of the plasma for the roughly treated sample.[51] These results demonstrated the versatility of the proposed sensor for detecting Hg^{2+}, even in natural media.

As demonstrated above, the turn-off sensor possessed better sensitivity than other reported chip-based Hg^{2+} sensors as well as great selectivity and reliability for practical applications. However, turn-off sensors are usually prone to false-positive signals. In order to overcome this problem, the sensor was turned into a turn-on sensor by adopting a three-strand design as shown in Figure 5. A Cy5-tagged short oligonucleotide strand, probe B′, was complementary to the 5′-end of probe A′, and a quencher (BHQ3)-tagged polyadenine strand, probe C′, was hybridized with probe A′ next to probe B′, forming a low-fluorescence chip ready for Hg^{2+} detection. The typical scanometric images of the slide after immobilization of probe A′, hybridization with probe B′, hybridization with probe C′, and subsequent exposure to a Hg^{2+} solution are shown in Figure 5B. After the immobilization of probe A′ and the hybridization of probe B′ with Cy5 labeled, the slide showed

dx.doi.org/10.1021/ac301954j | Anal. Chem. 2012, 84, 8060−8066

strong fluorescence. Then BHQ3-labeled probe C′ was hybridized with probe A′ and a fluorescence resonance energy transfer (FRET) process between the fluorophore (Cy5) and quencher (BHQ3) occurred, resulting in a 90% fluorescence intensity decrease in the spots. As expected, the fluorescence intensity was brought back to 100% after the chip was exposed to the 100 μM Hg^{2+} solution.

The turn-on sensor turned out to be quite sensitive, as shown in Figure 6; as little as 8.6 nM Hg^{2+} was able to be detected

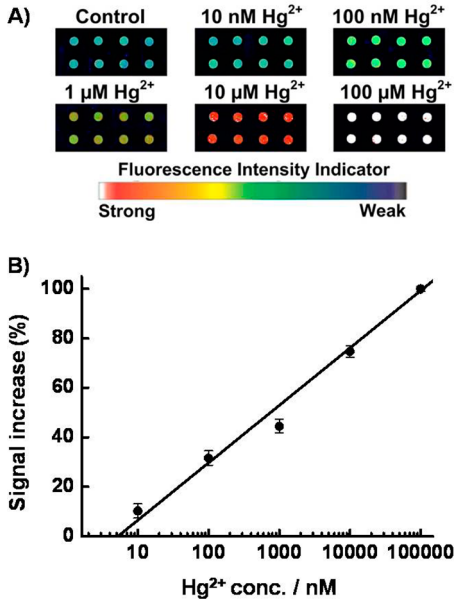

Figure 6. (A) Scanometric images of the turn-on chip in the presence of various concentrations of Hg^{2+} in the buffer. (B) The percentage of fluorescence intensities increases as a function of the Hg^{2+} concentration in the buffer.

with a dynamic range of more than 4 orders of magnitude. A fairly good linear response was observed with correlation efficiencies of 0.99 for the whole detection range. The sensitivity of the sensor could be further improved by optimizing the probe lengths and base compositions to further decrease the background signal. The turn-on sensor still kept the great selectivity as that of the turn-off sensor. In contrast to significant fluorescence increase (74.7 ± 2.4%) as observed in the presence of 10 μM Hg^{2+}, very little change (<6.5%) of the fluorescence intensity was observed upon exposure to other metal ions at the same concentration (Figure 7). The practical application of the turn-on sensor was also tested by detecting a spiked-in mercury ion in drinking water. No difference in the fluorescence intensity changes was found between the standard samples containing Hg^{2+} at 0.5 μM (or 5 μM) in the buffer and drinking water spiked with equivalent amounts of Hg^{2+}. The scanometric images and quantitative fluorescence changes can be found in Figure S-4A,B of the Supporting Information.

CONCLUSIONS

In summary, we have developed two ready-to-use, highly sensitive, and highly selective chip-based fluorescent sensors for Hg^{2+} detection. The detection mechanism is mainly based on the selective T−Hg^{2+}−T coordination between two neighboring poly-T strands and its induced displacement of the fluorophore- or quencher-labeled poly-A strand in the turn-off and turn-on platform, respectively. Compared to the signal-

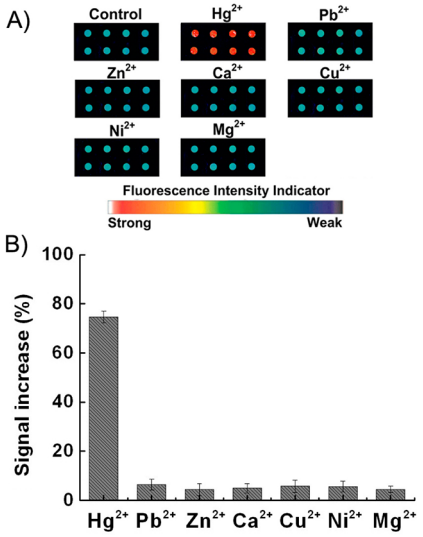

Figure 7. (A) Scanometric images of the turn-on chip in the presence of various metal ions at a concentration of 10 μM. (B) The percentage of fluorescence intensities increases as a function of various metal ions.

on sensor, the signal-off sensor is simpler for fabrication and does not require probe optimization. However, the signal-on sensor can prevent false-positive signals. It should be pointed out that poly-T, instead of poly-A, should be immobilized on the chip to meet the requirement of probe proximity for effective T−Hg^{2+}−T coordination between two neighboring poly-T strands. The turn-off sensor with the poly-A strand immobilized on the surface exhibited an ∼100-fold increase in the detection limit (∼100 nM, data not shown). The significant decrease in the sensitivity for the reversed design is quite understandable because the density of the hybridized poly-T is much lower than the density of the surface-immobilized poly-T in our demonstrated turn-off sensor, resulting in a much less efficient formation of T−Hg^{2+}−T between two poly-T strands. However, this much less sensitive reversed design can be used as a control to exclude the possibility of false-positive signals, which have great importance for the practical uses of turn-off sensors. For example, the reversed design and our original design would produce a similar signal decrease under denaturing conditions. In contrast, in the presence of Hg^{2+}, the reversed sensor would produce a much smaller signal decrease. In this way the false-positive signals can be easily excluded. Both the turn-on and the turn-off sensors described in this study offer many properties desired for on-site practical applications: high sensitivity, high selectivity, good stability, speed, no need for complicated instrumentation, and operational convenience.

ASSOCIATED CONTENT

Supporting Information

Additional fluorescence emission spectra and scanometric images of kinetic experiments and detection of Hg^{2+} in drinking water and fresh milk. This material is available free of charge via the Internet at http://pubs.acs.org.

AUTHOR INFORMATION

Corresponding Author

*E-mail: xlou9999@yahoo.com. Tel: +86-10-68902491, ext. 808. Fax: +86-10-68902320.

Author Contributions

[⊥]Authors contributed equally to this work.

Notes

The authors declare no competing financial interest.

■ ACKNOWLEDGMENTS

This work was supported by the National Natural Science Foundation (Grant 20975108), the 973 Program of the Ministry of Science and Technology of China (Grants 2012CB933303 and 2011CB707505), the Beijing City Board of Education Science and Technology Program (Grant KM201210028020), the Scientific Research Foundation for the Returned Overseas Chinese Scholars, the State Education Ministry, the Beijing City Talent Training Aid Program (Grant 2012D005016000004), the National Key Technology R&D Program (Grant 2012BAK08B05), and the Science and Technology Commission of Shanghai Municipality (Grants 11391901900, 11530700800, 11ZR1443900, and 10391901600).

■ REFERENCES

(1) Zahir, F.; Rizwi, S. J.; Haq, S. K.; Khan, R. H. *Environ. Toxicol. Pharmacol.* **2005**, *20*, 351−360.
(2) Magos, L.; Clarkson, T. W. *Ann. Clin. Biochem.* **2006**, *43*, 257−268.
(3) Leermakers, M.; Baeyens, W.; Quevauviller, P.; Horvat, M. *TrAC, Trends Anal. Chem.* **2005**, *24*, 383−393.
(4) Guo, X.; Qian, X.; Jia, L. *J. Am. Chem. Soc.* **2004**, *126*, 2272−2273.
(5) Nolan, E. M.; Lippard, S. J. *Chem. Rev.* **2008**, *108*, 3443−3480.
(6) Tang, Y.; He, F.; Yu, M.; Feng, F.; An, L.; Sun, H.; Wang, S.; Li, Y.; Zhu, D. *Macromol. Rapid Commun.* **2006**, *27*, 389−392.
(7) Chen, P.; He, C. A. *J. Am. Chem. Soc.* **2004**, *126*, 728−729.
(8) Ono, A.; Togashi, H. *Angew. Chem., Int. Ed.* **2004**, *43*, 4300−4302.
(9) Liu, X.; Tang, Y.; Wang, L.; Zhang, J.; Song, S.; Fan, C.; Wang, S. *Adv. Mater.* **2007**, *19*, 1471−1474.
(10) Yuan, M.; Zhu, Y.; Lou, X.; Chen, C.; Wei, G.; Lan, M.; Zhao, J. *Biosens. Bioelectron.* **2012**, *31*, 330−336.
(11) Liu, J.; Lu, Y. *Angew. Chem., Int. Ed.* **2007**, *46*, 7587−7590.
(12) Matsushita, M.; Meijler, M. M.; Wirsching, P.; Lerner, R. A.; Janda, K. D. *Org. Lett.* **2005**, *7*, 4943−4946.
(13) Wang, Z.; Lee, J. H.; Lu, Y. *Chem. Commun.* **2008**, *45*, 6005−6007.
(14) Ye, B. C.; Yin, B. C. *Angew. Chem., Int. Ed.* **2008**, *120*, 8514−8517.
(15) Freeman, R.; Finder, T.; Willner, I. *Angew. Chem., Int. Ed.* **2009**, *48*, 7818−7821.
(16) Liu, C. W.; Huang, C. C.; Chang, H. T. *Anal. Chem.* **2009**, *81*, 2383−2387.
(17) Ren, X.; Xu, Q. H. *Langmuir* **2009**, *25*, 29−31.
(18) Zhang, X.; Li, Y.; Su, H.; Zhang, S. *Biosens. Bioelectron.* **2009**, *25*, 1338−1343.
(19) Dave, N.; Chan, M. Y.; Huang, P. J. J.; Smith, B. D.; Liu, J. *J. Am. Chem. Soc.* **2010**, *132*, 12668−12673.
(20) Zhu, X.; Zhou, X.; Xing, D. *Biosens. Bioelectron.* **2011**, *26*, 2666−2669.
(21) Lee, J. S.; Han, M. S.; Mirkin, C. A. *Angew. Chem., Int. Ed.* **2007**, *46*, 4093−4096.
(22) Li, D.; Wieckowska, A.; Willner, I. *Angew. Chem., Int. Ed.* **2008**, *120*, 3991−3995.
(23) Wang, H.; Wang, Y.; Jin, J.; Yang, R. *Anal. Chem.* **2008**, *80*, 9021−9028.
(24) Xue, X.; Wang, F.; Liu, X. *J. Am. Chem. Soc.* **2008**, *130*, 3244−3245.
(25) Li, L.; Li, B.; Qi, Y.; Jin, Y. *Anal. Bioanal. Chem.* **2009**, *393*, 2051−2057.
(26) Li, T.; Dong, S.; Wang, E. *Anal. Chem.* **2009**, *81*, 2144−2149.
(27) Xu, X.; Wang, J.; Jiao, K.; Yang, X. *Biosens. Bioelectron.* **2009**, *24*, 3153−3158.
(28) Kong, R. M.; Zhang, X. B.; Zhang, L. L.; Jin, X. Y.; Huan, S. Y.; Shen, G. L.; Yu, R. Q. *Chem. Commun.* **2009**, *2009*, 5633−5635.
(29) Liu, S. J.; Nie, H. G.; Jiang, J. H.; Shen, G. L.; Yu, R. Q. *Anal. Chem.* **2009**, *81*, 5724−5730.
(30) Zhu, Z.; Su, Y.; Li, J.; Li, D.; Zhang, J.; Song, S.; Zhao, Y.; Li, G.; Fan, C. *Anal. Chem.* **2009**, *81*, 7660−7666.
(31) Wu, D.; Zhang, Q.; Chu, X.; Wang, H.; Shen, G.; Yu, R. *Biosens. Bioelectron.* **2010**, *25*, 1025−1031.
(32) Gerhold, D.; Rushmore, T.; Caskey, C. T. *Trends Biochem. Sci.* **1999**, *24*, 168−173.
(33) Zhu, H.; Snyder, M. *Curr. Opin. Chem. Biol.* **2003**, *7*, 55−63.
(34) Anzenbacher, P.; Liu, Y. L.; Kozelkova, M. E. *Curr. Opin. Chem. Biol.* **2010**, *14*, 693−704.
(35) Goodey, A.; Lavigne, J. J.; Savoy, S. M.; Rodriguez, M. D.; Curey, T.; Tsao, A.; Simmons, G.; Wright, J.; Yoo, S. J.; Sohn, Y.; Anslyn, E. V.; Shear, J. B.; Neikirk, D. P.; McDevitt, J. T. *J. Am. Chem. Soc.* **2001**, *123*, 2559−2570.
(36) Bi, X. Y.; Agarwal, A.; Yang, K. L. *Biosens. Bioelectron.* **2009**, *24*, 3248−3251.
(37) Dalavoy, T. S.; Wernette, D. P.; Gong, M.; Sweedler, J. V.; Lu, Y.; Flachsbart, B. R.; Shannon, M. A.; Bohn, P. W.; Cropek, D. M. *Lab Chip* **2008**, *8*, 786−793.
(38) Swearingen, C. B.; Wernette, D. P.; Cropek, D. M.; Lu, Y.; Sweedler, J. V.; Bohn, P. W. *Anal. Chem.* **2005**, *77*, 442−448.
(39) Zuo, P.; Yin, B. C.; Ye, B. C. *Biosens. Bioelectron.* **2009**, *25*, 935−939.
(40) Lee, J.; Kim, H. J.; Kim, J. *J. Am. Chem. Soc.* **2008**, *130*, 5010−5011.
(41) Lee, J.; Jun, H.; Kim, J. *Adv. Mater.* **2009**, *21*, 3674−3677.
(42) Wu, C. M.; Lin, L. Y. *Biosens. Bioelectron.* **2004**, *20*, 864−871.
(43) Lee, J. S.; Mirkin, C. A. *Anal. Chem.* **2008**, *80*, 6805−6808.
(44) Palomares, E.; Vilar, R.; Durrant, J. R. *Chem. Commun.* **2004**, 362−363.
(45) Miyake, Y.; Togashi, H.; Tashiro, M.; Yamaguchi, H.; Oda, S.; Kudo, M.; Tanaka, Y.; Kondo, Y.; Sawa, R.; Fujimoto, T.; Machinami, T.; Ono, A. *J. Am. Chem. Soc.* **2006**, *128*, 2172−2173.
(46) Tanaka, Y.; Oda, S.; Yamaguchi, H.; Kondo, Y.; Kojima, C.; Ono, A. *J. Am. Chem. Soc.* **2007**, *129*, 244−245.
(47) Liu, M. Y.; Lou, X. H.; Juan, D.; Guan, M.; Wang, J.; Ding, X. F.; Zhao, J. L. *Analyst (Cambridge, U.K.)* **2012**, *137*, 70−72.
(48) Ono, A.; Miyake, Y. *Nucleic Acids Res. Suppl.* **2003**, *3*, 227−228.
(49) Widengren, J.; Schwilles, P. *J. Phys. Chem. A* **2000**, *104*, 6416−6428.
(50) Ataro, A.; McCrindle, R. I.; Botha, B. M.; McCrindle, C. M. E.; Ndibewu, P. P. *Food Chem.* **2008**, *111*, 243−248.
(51) Korn, M. D. A.; Morte, E. S. D.; dos Santos, D.; Castro, J. T.; Barbosa, J. T. P.; Teixeira, A. P.; Fernandes, A. P.; Welz, B.; dos Santos, W. P. C.; dos Santos, E.; Korn, M. *Appl. Spectrosc. Rev.* **2008**, *43*, 67−92.